Controlling laser ablation plasma with external electrodes

- Application to sheath dynamics study and beam physics -

Fumika Isono, Mitsuo Nakajima, Jun Hasegawa, Tohru Kawamura, and Kazuhiko Horioka

Department of Energy Sciences, Tokyo Institute of Technology,
Nagatsuta 4259, Midori-ku, Yokohama, 226-8502, Japan

ABSTRACT

The potential of laser ablation plasma was controlled successfully by using external ring electrodes. We found that an electron sheath is formed at the plasma boundary, which plays an important role in the potential formation. When the positively biased plasma reaches a grounded grid, electrons in the plasma are turned away and ions are accelerated, which leads to the formation of a virtual anode between the grid and an ion probe. We think that this device which can raise the plasma potential up to order of kV can be applied to the study of sheath dynamics and to a new type of ion beam extraction.

Keywords

laser ablation plasma, sheath, space charge limited current, virtual anode, beam extraction

1 Introduction

Since laser ablation plasma expands with extensive velocity and density, and can be produced from almost any kind of solid target, it has been applied to various industrial fields, such as Laser Ion Source, complex thin films made by Pulsed Laser Deposition, plasma etching and surface modification [1] [2].

Laser-produced plasma drifts adiabatically with its pressure gradient under the given boundary conditions. However, its dynamics when electric forces have been applied has not been clarified thoroughly yet. In this study, electric fields are applied to the drifting plasma, detached from the plasma boundary. Therefore, boundary conditions such as electrodes and walls give conditions to the plasma about how to raise self-consistent potential which affect the transportation of ions in plasma. When plasma touches a wall, it keeps quasi-neutrality by forming a sheath which balances the total electron current and the ion current flowing toward the wall, and the plasma potential needs to be determined by the sheath currents.

We have investigated the behavior of plasma by changing the external environment, and succeeded in raising the bulk plasma potential up to 1 kV by using external electrodes. This control was achieved because of the stable formation of an electron sheath in front of the electrode.

This device which can control plasma potential is useful for the research of plasma dynamics. With this device we observe the formation of sheaths, and an virtual anode formed by the extraction of ions from plasma.

In the end, we will show that we can extract a stable ion beam which is not affected by the ion current supply similar to the grid

controlled ion extraction [3].

2 Sheath

2.1 Interaction between bulk plasma and walls

When plasma touches a wall, a boundary called sheath is formed between the wall and plasma, and the total amount of electron current flowing to walls becomes equal to ion current so that plasma can ensure quasi-neutrality [4].

In general, positive charges remain in bulk plasma, and make the potential higher than the wall potential by forming an ion sheath at the edges because of small inertia of an electron. In this way, the total electron current balances an ion current flowing toward the walls.

For plasma between two walls, the bulk plasma potential approaches to that of the wall where electrons can flow easily, i.e. a positively biased wall, and ion sheaths are usually formed at the both sides of walls.

However, if the electron current is limited in some situations, for example, the positively biased wall is small and/or the wall is distant from the plasma core, the plasma potential becomes lower than that of the wall and forms an electron sheath. When the loss areas of ions and the electrons are different, the existence of an electron sheath is provided around the condition of Eq. (1) [6].

$$\frac{A_\mathrm{i}}{A_\mathrm{e}} \gtrapprox \sqrt{\frac{m_\mathrm{i}}{m_\mathrm{e}}} \tag{1}$$

2.2 Space charge limited current

One-dimensional space charge limited current when charged particles are emitted with zero velocity is obtained by solving Poisson's equation

$$\frac{\mathrm{d}^2\phi}{\mathrm{d}x^2} = -\frac{\rho}{\varepsilon_0} \tag{2}$$

with a boundary condition

$$V = 0 \text{ and } \mathrm{d}V/\mathrm{d}x = 0 \text{ at } x = 0,$$
$$V = V_0 \text{ at } x = a. \tag{3}$$

Then, the following Child equation is derived.

$$J = 4\varepsilon_0/9\sqrt{2em}{V_0}^{3/2}/a^2 = \chi {V_0}^{3/2}/a^2 \tag{4}$$

where ρ is charge density and χ is a constant number.

When the condition $\mathrm{d}V/\mathrm{d}x = 0$ at the emitter is retained, but in which the emitted particles are all given in an initial velocity v_0

$$V = V_0 = m{v_0}^2/2e \text{ at } x = 0, \tag{5}$$

we obtain the relation between potential V at distance x and current density J from Eq. (2).

$$(\sqrt{V/V_0} - 1)^{1/2}(\sqrt{V/V_0} + 2){V_0}^{3/4}$$
$$= (3x/2)(m/2e)^{1/4}(J/\varepsilon_0)^{1/2} \tag{6}$$

Figure 1 shows the schematic diagram of a spatial potential profile between a grid and an ion collector. When plasma with a negative potential relative to the grid reaches the grid, electrons are turned away, and an ion sheath is formed in front of the grid.

On the other hand, ions are accelerated, and they pass though the grid. Thus, three types of potential profiles shown in Fig. 1 can be formed between the grid and the ion collector which is placed at $x = a$.

In Case 1, potential gradient is negative at $x = 0$, and all ions with initial velocity are accelerated through the path.

In Case 2, potential has a peak between the two planes, but all the current flows into the ion collector. Potential distributions in both

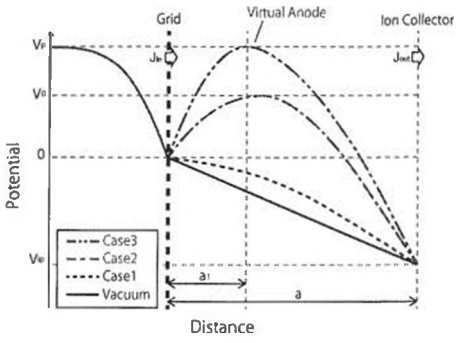

Figure 1: Schematic diagram of a spatial potential profile between a grid and an ion collector.

areas, the left and the right side of the peak, follow Eq. (6). Since the current in these two areas is same, we can obtain the maximal value and the position from a given injected current.

In Case 3, the maximum potential reaches plasma potential V_p. The maximum acts as a virtual emission-limited anode emitter, and reflects the portion of the current. Both boundaries of two areas separated at the virtual emitter are equal to the boundary condition (3). Since Poisson's equation is about the distribution of charges, the sum of the absolute value of injected current and reflected current is equal to space charge limited current even though opposing current flows in the left area of the virtual anode. In the result, current in both areas is space charge limited, and can be solved by using two equations given by the Child equation (4), where transmission of a current is $J_{out} = \alpha J_{in}$, $0 < \alpha < 1$.

$$\begin{cases} J_{in} + (1-\alpha)J_{in} = \chi V_p^{3/2}/{a_1}^2 \\ J_{out} = \alpha J_{in} = \chi(V_p - V_{ip})^{3/2}/(a-a_1)^2 \end{cases} \quad (7)$$

Now we think that ions with an ion current density signal shown in Fig. 2(a) is injected from the left side of the grid as shown by J_{in} in Fig. 1. The current is assumed to be one-dimensional and static, and transition time is

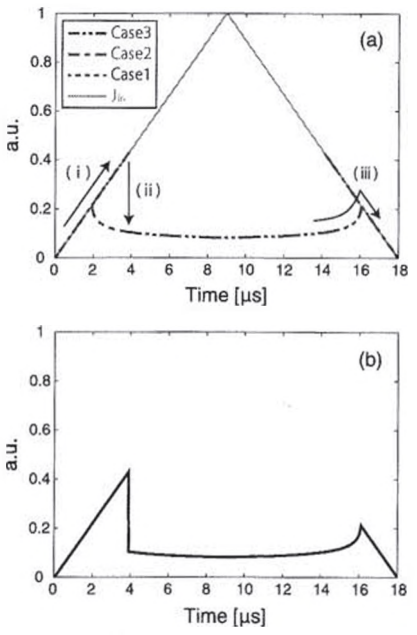

Figure 2: (a) Injected current density J_{in} and transitions of emission current density J_{out}, (b) Emission current density J_{out}.

neglected for simplicity. The potential between the two planes changes depending on the time change of injected current density J_{in} as below.

i. While the injected current increases, the potential profile between the grid and the ion collector transits from Case 1 to Case 2. The peak of the potential appears in Case 2, and its value V_0 will increase until a maximum value called V_m .

ii. When V_0 is near V_m, the current is in bistable condition, where the potential profile can take either of Case 2 and Case3. The profile transits from Case 2 to Case 3 when the current reaches the maximum of Case 2. Note that ion current J_{out} which is collected at the ion collector in Case 3 is less than the maximum of J_{out} in Case 2. If the injected current J_{in} then decreased, the distance of virtual anode from the grid a_1 shifts toward the

ion collector and the transmitted current J_{out} will increase.

iii. For the further decrease of J_{in}, the current becomes bistable condition again. The potential profile transits from Case 3 to Case 2 when reflection of the current is ceased, or the operation mode goes back to just before it happens.

As shown above, the potential transforms from Case 1 → Case 2 → Case 3 → Case 2 → Case 1, and the current has a bistable solution when the transition between Case 2 and Case 3 occurs. The signal of current density J_{out} observed at the ion current is predicted to be like Fig. 2(b).

3 Experimental setup

Figure 3 illustrates the schematic drawing of the apparatus. A copper target inside a vacuum chamber was irradiated with a KrF excimer laser (λ = 248nm) at an incident angle of 70° . The irradiation power density was $10^8 \sim 10^9$ W/cm^2 and the pressure inside the chamber was 10^{-4} Pa. Plasma made by the laser ablation drifts toward electrodes while expanding. A tantalum aperture with a diameter of 2 mm was placed in front of the target to limit the angle of plasma so that the plasma doesn't touch electrodes.

The cross-sectional diagram of external electrode is shown in Fig. 4. 4 mm-thick, 32 mm inner diameter ring electrodes and ring insulators were lined up alternately. Electrodes can change external electric field which interacts with the drifting plasma. A voltage in the range of 0 ∼ +1 kV was applied to the electrodes. Langmuir probe was inserted 20 mm before the grid, between 4th and 5th electrodes from the target on a cylindrical axis. The

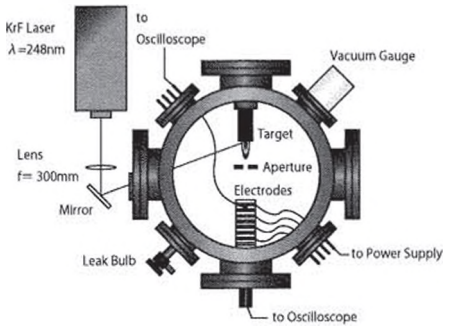

Figure 3: Schematic drawing of the experimental apparatus.

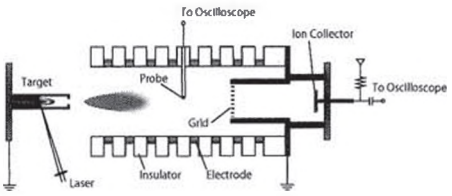

Figure 4: Cross-sectional diagram of electrodes.

probe can measure the plasma potential via a high voltage probe with the input impedance of 100 MΩ.

A 100 mesh grid was placed 81 mm from the target at a side of grounded thimble on the downstream side of the electrodes. An ion collector was biased at -100 V to measure an ion current signal and its distance from the grid a can be changed.

When the plasma potential was measured, the voltage was applied to six electrodes on the left side in Fig. 4. When an ion current was measured, it was applied to the very left side of the electrode which was placed 24 mm from the target. From now, we call the voltage applied electrode " control electrode " . The other electrodes were grounded.

4 Results and Discussions

4.1 controlling the plasma potential

Figure 5 shows the time evolution of plasma potential when a DC voltage was applied to the control electrodes up to +1 kV. We can see that the plasma potential had more than 80 percent of the control electrodes' potential.

The plasma potential becomes close to the potential of the wall where electrons are easy to escape. We consider that the plasma potential rises when the plasma plume is detached from the grounded target and electrons become easier to escape toward the control electrodes.

Once the plasma potential has been raised, electrons can not escape to the grounded grid. When the plume reaches the grid, an ion sheath is formed in front of the grid. At this time, all ions escaping from the plasma core go to the grid and the ion collector, while all electrons escaping from the plasma core go to the control electrodes. We think that the electron sheath and the ion sheath balanced the total electron current and the ion current flowing toward walls, which determined and maintained the plasma potential as shown in Fig. 5.

Note that the plasma potential might not be measured correctly at the beginning of the signal due to dilute plasma at that time.

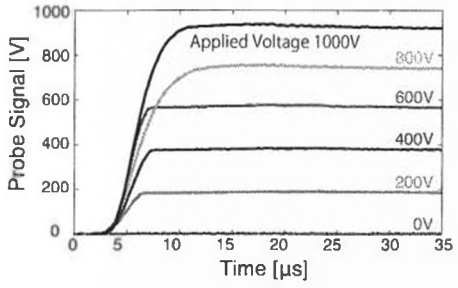

Figure 5: Time evolution of plasma potential when a positive voltage is applied to the control electrodes.

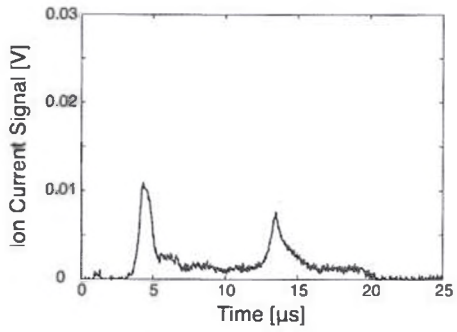

Figure 6: The ion current signal when 80 V is applied to the control electrode (a =29.5 mm).

4.2 Extraction of ions from plasma

Figure 6 shows the typical ion current signal measured with the ion collector when a positive voltage was applied to the control electrode. Peaks were formed at the beginning and the end of the signal, and the current was suppressed between these two peaks. The second peak is needed to be examined more as we discuss later.

Next, we changed the distance of the ion collector from the grid a, and the voltage applied to the grid under the condition of higher laser irradiation power density. Figure 7 shows the ion current signal when the applied voltage was changed with distance a fixed to 10 mm. In this high plasma flux condition, we can see that Case 3 dominated over Case 2. A flat part appeared in the signal and the value seemed to be gained with the increase of the applied voltage. Here we know that only ions reached the ion collector because the current signal was not changed even though a positive voltage 31.7 V was applied to the ion collector.

Figure 8 shows the ion current signal when the distance a was changed and the applied voltage was fixed to 300 V. We can see that the current was gained with the decrease of distance a from Fig. 8(a). Furthermore,the

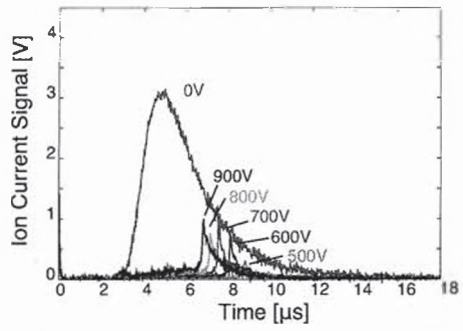

Figure 7: Ion current signals when a positive voltage is applied to the control electrode (a =10 mm).

minima of the flat part of the signal fitted a a^{-2} scaling as shown in Fig. 8(b).

Because the flat part of the signal was gained with the increase of the applied voltage and was inversely proportional to the square of distance a, we can say that the formation of a virtual anode is the reason why the flat part was shown. Furthermore, the virtual anode was formed during the increase of injected current and collapsed during the decrease of injected current as seen in Figs. 6 $\sim$ 8. However, the right peak of the the ion current signal has a rapid rise although it has to be Case 3, in which the virtual anode is still to be formed. At this time, almost all current is reflected at the virtual anode because of the large injected current. This dynamics of the injected current might be the cause of this early collapse. Further investigation is needed to clarify the reasons why the virtual anode collapsed early and the current was decreased after the right peak.

From the results above, the potential profile of plasma while ions were extracted in this apparatus is assumed to be like Fig. 9. An electron sheath was formed in front of the electrode where the positive voltage was applied, and plasma with positive potential formed an

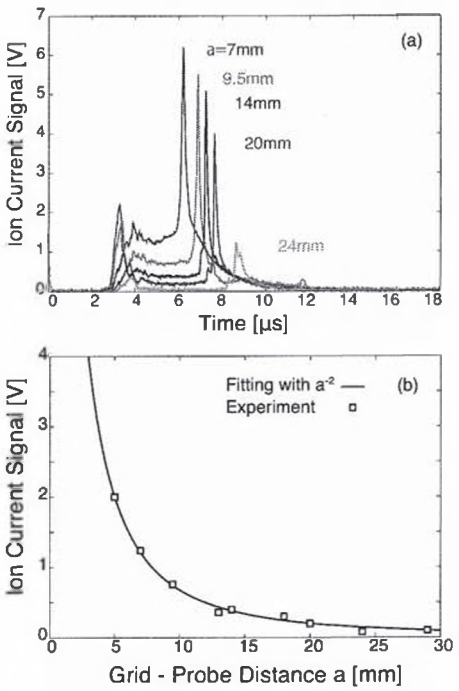

(a) Ion current signals at a = 7 $\sim$ 24mm when 300 V is applied to the control electrode
(b) Ion current signal follows a^{-2} rule

Figure 8: Relation between Ion current and distance a.

ion sheath in front of the grid. Then after the extraction of ions at the grid, a virtual anode was formed between the grid and the ion collector.

5 Conclusion

We succeeded in controlling the potential of laser ablation plasma up to order of kV. This was obtained by placing ring external electrodes away from plasma plume boundary so that the plasma could form an electron

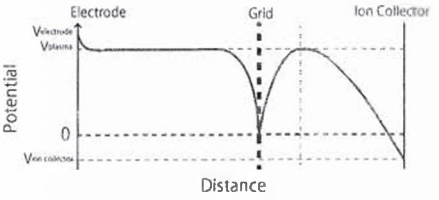

Figure 9: Schematic diagram of the spatial profile of the plasma and ion potential at the whole apparatus.

sheath in front of the electrodes. When the plasma reached a grounded grid, an ion sheath was formed in front of it besides the electron sheath.

One of the advantages this device has is that it can control the plasma potential easily because of the steady formation of an electron sheath. Since the mass of electrons is much smaller than that of ions, we could raise the plasma potential even though there is a distance between plasma and electrodes. This distance makes this device durable for a destructive electric discharge. Another advantage is that this potential controlled plasma is unlikely to be affected by the discharge for the plasma production because the time scale for the laser irradiation is much shorter than the plasma drifting and adiabatic expansion time. We think that this simple and calm device would become useful for the research of sheath dynamics.

Using this device, we observed the formation of a virtual anode. We found that the virtual anode was collapsed during the decrease of injected current, and the timing was dependent on a reflected current growth.

Also, it became clear that we can obtain flat ion current when the virtual anode is formed. By utilizing this potential raising method, we expect that a new type of ion beam extraction will become possible as a replacement of grid controlled ion extraction [3] in which a destructive electric discharge is likely to happen. The challenges for the future would be the further investigation of beam physics using potential controlled plasma source, including the dynamical behavior of unstable virtual anode.

References

[1] Frederick P. Boody, Reinhard Hpfl, Heinrich Hora and Jak C. Kelly, Laser and Particle Beams, **14**, 443-448 (1995).

[2] P. R. Willmott and J. R. Huber, Reviews of Modern Physics, **72**, 315-328 (2000).

[3] S. Humphries, C. Burkhart, S. Coffey, G. Cooper, K. Len, M. Savage and D. M. Woodall, Journal of Applied Physics, **59**, 1790-1798 (1986).

[4] H. M. Mott-Smith and Irving Langmuir, Physical Review, **28**, 727-763 (1926).

[5] J. Loizu, J. Dominski, P. Ricci and C. Theiler, Physics of Plasmas, **19**, 083507, 1-7 (2012).

[6] Noah Hershkowitz, Physics of Plasmas, **12**, 055502, 1-11 (2005).

[7] A. Theodore Forrester, "Large ion beams: fundamentals of generation and propagation", 5-22, Wiley, California (1988).